



Full Length Article

Fluidised bed combustion and ash fusibility behaviour of coal and spent coffee grounds blends: CO and NO_x emissions, combustion performance and agglomeration tendency

Eduardo Garcia^a, Manuel F. Mejía^b, Hao Liu^{a,*}

^a Faculty of Engineering, University of Nottingham, University Park, Nottingham, UK

^b Faculty of Engineering, Central University, Bogotá, Colombia



ARTICLE INFO

Keywords:

Co-combustion
Biomass blending ratio
Spent coffee grounds
Fluidized bed combustion
Agglomeration
Combustion performance

ABSTRACT

The co-combustion of coal and waste biomass is an advantageous option for combined waste biomass disposal and energy production. However, co-firing coal with waste biomass has to overcome various ash-related operational problems, for example, ash agglomeration and bed defluidisation in fluidised bed boilers. Using spent coffee grounds (SCG) for energy generation via co-combustion is much more sustainable and environmentally friendly than SCG disposal in landfills. The research done so far on the co-combustion of coal and SCG is quite scarce and almost non-existing. Further research is needed to understand how the properties of SCG affect the co-combustion of coal and SCG in existing coal-fired boilers. This study investigates the combustion of a bituminous coal blended with SCG in a pilot-scale (30kWth) bubbling fluidised bed (BFB) combustor focusing on CO and NO_x emissions, combustion performance, and agglomeration tendency. The BFB combustion tests were conducted at 900 °C and atmospheric pressure using silica sand as the bed material. For comparison purposes, combustion tests of the same coal in pure and blended with wheat straw pellets at the same blending ratio were also performed. Further, ash fusibility studies were performed to elucidate the interactions between the coal ash and SCG ash, and the effect of ash compositions on the fusibility temperatures. Samples of the used bed material collected from the combustor and cyclone ash were characterised by SEM-EDS and XRF. The BFB combustion test results revealed that SCG could reduce the efficiency loss of coal combustion under co-combustion conditions. Despite the higher K₂O content in SCG compared to wheat straw, a reduced agglomeration tendency was observed with the BFB combustion of the coal-SCG blends. The results from the characterisation of the used bed material, cyclone ash, and ash fusibility studies confirmed this finding, which was attributed to the formation of high melting temperatures Mg- and Ca-bearing compounds.

1. Introduction

Coal has long been the predominant fuel for electricity and heat generation worldwide [1]. Although coal-fired power generation has decreased in the United States and Europe in recent years, growths in China, India, and other parts of Asia kept coal as the largest source of power generation with a share of 36 % in 2018 [2]. Greenhouse gas (GHG) emissions from burning coal are believed to be the major contributor to the global climate change, and responsible for 30% of all energy-related (CO₂) emissions, exceeding 10 Gt CO₂ in 2018 [1]. Despite the general interest in reducing the share of coal usage and switching to low-carbon technologies, coal has been projected to remain

a key resource in the world energy mix in the coming decade [3-5]. Therefore, the implementation of more sustainable alternatives for coal is a priority task for the coal-fired power industry.

The co-combustion of coal and waste biomass is considered an advantageous option for combined waste biomass disposal and energy production for stationary applications [6]. It represents a low-cost alternative to the use of dedicated waste biomass combustion plants and a sustainable option with the potential to achieve significant reductions in the emissions of CO₂ and various pollutants (NO_x and SO₂ etc.) per unit of energy generated compared to exclusive coal combustion [7,8]. However, coal and waste biomass have significant differences in combustion and devolatilisation behaviours, char reactivity, and ash

* Corresponding author.

E-mail address: liu.hao@nottingham.ac.uk (H. Liu).

<https://doi.org/10.1016/j.fuel.2022.125008>

Received 23 December 2021; Received in revised form 2 May 2022; Accepted 21 June 2022

Available online 28 June 2022

0016-2361/© 2022 The Author(s). Published by Elsevier Ltd. This is an open access article under the CC BY license (<http://creativecommons.org/licenses/by/4.0/>).

characteristics [9,10]. These differences can not only affect the co-combustion performance of the coal and waste biomass blends but also result in additional ash-related operational problems to the co-combustion boiler.

Coffee is an important industrial sector in about 80 countries, and one of the most popular beverages and the second largest traded commodity after petroleum [11-16]. Global coffee consumption has been increasing annually, with more than 9.9 billion kilograms consumed in 2021 [17]. The spent coffee grounds (SCG) consist of the grinds remaining after the extraction of desirable compounds with hot water to produce a coffee beverage or during the production of instant coffee preparations [18,19]. In average, processing one ton of unroasted coffee produces 650 kg of SCG [18,20]. SCG is a kind of waste biomass [21] and as biodegradable waste, its disposal in landfills is strongly discouraged in the European union. However, landfilling of SCG is still a common practice in developing countries around the world [22]. The economic cost and environmental consequences of disposing SCG in this way are undesirable, and for this reason, better alternative methods to deal with SCG need to be developed and sought [19]. Combustion and composting are the other two traditional treatment/disposal methods sporadically practiced by the coffee industry [22]. SCG has been partially used as fuel in boilers of the same industry for either heat or power generation, but a greater part of this material is often accumulated as waste [23,24].

Some researchers have studied the potential of SCG as fuel using various combustion technologies. Limousy et al. [14,25] and Jeguirim et al. [26] studied the combustion of SCG in pure form and blends with sawdust and coffee husk using a residential wood pellet boiler. Byul, et al. [27] investigated the combustion of SCG in a fixed bed boiler (6.5 kW) in terms of the gaseous emissions. Nosek, et al. [21] studied the use of SCG as fuel in pure and blends with sawdust using a fixed bed boiler (18 kW). Kim et al. [17] investigated the combustion of SCG briquettes in terms of emissions and shape retention compared to anthracite briquettes. Colantoni et al. [16] studied the combustion of pellets made of pure SCG and SCG blended with sawdust using a fixed bed boiler (80 kW). So far, few have investigated the combustion of coal blended with SCG at high blending ratios. Since the heating value of SCG is similar to those of low-rank coals, burning coal blended with SCG at high blending ratios should not lead to an obvious output reduction of the co-firing boiler while achieving more substantial CO₂ emission reductions. However, SCG properties and its ash characteristics may pose technological challenges and hinder the use of SCG in co-combustion applications. These challenges are mostly linked to the thermal behaviour, high quantities of alkali and alkaline metals species in the biomass ash, and the lower ash melting temperatures in comparison to coal ash. Several studies have focused on the effect of ash composition on the ash fusibility characteristics of coal [28], biomass [29-31], and coal and biomass blends [32-35]. But so far little has been reported about the SCG ash composition and its effect on ash fusibility temperatures (AFT) when used in pure or blended with coal.

Fluidised bed combustion boilers have a unique advantage in fuel flexibility and hence are well-placed to co-fire coal blended with waste biomass at high blending ratios. However, ash agglomeration is a well-known operational issue associated with the combustion of biomass in fluidised bed boilers [36,37]. Ash agglomeration can lead to bed defluidisation and consequently the shutdown of the fluidised bed combustion plant. Few have investigated the combustion of SCG in blends with bituminous coals, which are the predominant fuel in the power sector [1,4,38]. In fact, to the best of the authors' knowledge, no one seems to have specifically investigated the effect of blending SCG with a bituminous coal on the combustion performance, agglomeration tendency in a fluidised bed boiler/combustor, and the ash fusibility characteristics of the coal-SCG blends. Therefore, this study was initiated to investigate the combustion of a bituminous coal blended with SCG in terms of the most representative flue gas emissions (i.e. CO, and NO_x), combustion performance, and agglomeration tendency in a pilot-scale fluidised bed combustor and the effect of ash composition of the

blends on the ash fusibility characteristics. For comparison purposes, combustion tests of the same coal in pure and blended with wheat straw pellets at the same blending ratio were also carried out.

2. Experimental

2.1. Fuels and materials

The bituminous coal used in this study was the same coal used for combustion in the industrial-scale fluidised bed boiler at the Newark Factory of British Sugar plc in the UK. It was supplied as 'washed singles' with 90 wt% of the particle size within the range of 12.5 mm and 28 mm. The spent coffee grounds were collected from a coffee shop at Jubilee Campus of the University of Nottingham, UK, whereas the wheat straw was supplied by Agripellets Ltd (UK) in the form of pellets with the average diameter of 6 ± 0.25 mm and length of 25 ± 5 mm. Table 1 shows the proximate and ultimate analyses of these fuels along with their heating values and ash compositions.

SCG has a lower level of ash content than wheat straw, 1.19 wt% and 6.23 wt%, respectively, but the SCG ash is mainly composed of basic oxides (K₂O, MgO, CaO, and P₂O₅), accounting for more than 92 wt% of the total ash, whereas the wheat straw (WS) ash is mainly composed of basic oxides (K₂O, and CaO) and SiO₂, accounting for more than 88 wt% of the total ash. The bituminous coal (BC) has an ash content of 7.99 wt %, which is similar to the wheat straw ash content, mainly composed of acidic oxides (SiO₂, Al₂O₃, and Fe₂O₃), accounting for more than 90 wt% of the total ash. In order to use the screw fuel feeding system to feed the bituminous coal to the bubbling fluidised bed (BFB) combustor used in this study, the received 'washed singles' of the bituminous coal were first crushed to smaller sizes and then sieved to obtain the coal particles within the size range of 12 mm and 20 mm for the scheduled combustion tests. A sample of 100 kg of raw spent coffee grounds, which had a moisture content of above 60 wt% when collected, was dried in the

Table 1

Proximate and Ultimate Analyses of the Fuels, their Heating Values, and Ash Compositions.

	BC ^a	SCG	WS
Proximate Analysis (wt%, dry basis)			
ash ^b	7.99	1.19	6.23
volatile matter (VM)	38.57	82.48	76.31
fixed carbon (FC) ^c	53.44	16.33	17.46
moisture (wt%, as received)	2.83	6.46	4.96
higher heating value ^d (HHV) (MJ/kg)	31.69	22.30	17.41
Ultimate Analysis (wt%, dry - ash - free basis)			
carbon	70.94	52.36	43.88
hydrogen	5.28	7.12	5.96
nitrogen	1.68	2.23	0.71
sulphur	1.23	0.12	0.58
oxygen ^c	20.87	38.17	48.87
Ash Analysis ^e (wt%)			
SiO ₂	43.21	0.00	64.69
P ₂ O ₅	0.27	18.40	2.82
Fe ₂ O ₃	11.84	0.52	0.42
Al ₂ O ₃	35.41	0.00	0.55
CaO	4.03	13.57	8.05
MgO	0.83	21.91	3.33
Na ₂ O	0.18	0.00	0.00
K ₂ O	0.90	38.20	16.18
SO ₃	2.28	6.84	2.29
Cl	0.00	0.20	1.60
TiO ₂	0.96	0.00	0.01

a. BC - bituminous coal, SCG - spent coffee grounds, WS - wheat straw.

b. the ashing temperature was 550 °C for spent coffee grounds and wheat straw, and 815 °C for bituminous coal according to BS/EN/ISO 18122:2015 and BS/ISO 1171:2010, respectively.

c. by difference.

d. Measured in an IKA C5000 Bomb Calorimeter on as received basis.

e. By X-ray Fluorescence (XRF) of the ashes from the feedstocks.

laboratory by natural air ventilation for up to 72 h and further in a muffle furnace if needed so that the moisture content was reduced to approximately 15 wt%, which was suggested as the optimum moisture content for biomass pellets manufacturing [39,40]. The reduction of the moisture content in the SCG from 15 wt% to 6.46 wt% (as shown in Table 1) corresponds to the moisture lost during the pelletisation of the SCG sample - further details on the manufacturing of SCG pellets will be given later in this section. The fuel blend reported in this study with the BFB combustion tests corresponded to the blend ratio of SCG pellets at 40 wt% in the bituminous coal (BC) – spent coffee grounds (SCG) mixture. The blend of BC with STW at the same proportion was tested in the BFB combustor for comparison purposes.

The silica sand (Garside 14/25) used in this study had a grain size ranging from 0.6 mm to 1.0 mm with a particle density of 2655 kg/m³. Detailed chemical analyses of the bed material are given in Table 2.

SCG pellets with an average diameter of 6 ± 0.25 mm and length of 20 ± 10 mm were manufactured in authors' own laboratory using a KL120B pellet machine. Fig. 1 shows the manufacturing progression of the SCG pellets. It is worth noting that during the SCG pellets manufacturing process, there was no need to add any binder. This was attributed to the high lignin content in SCG, which has been reported to be of up to 40 wt% [24,41]. Lignin is one of the traditional organic binders used in biomass densification [42]. Whittaker et al. [39] reported a strong positive relationship between pellet durability and lignin content in biomass densification tests. The suitability of the manufactured SCG pellets was confirmed by feeding tests with the screw feeder of the BFB combustor.

2.2. Fuel ash samples preparation

Ash samples of BC, WS, and SCG were produced in a Carbolite CFW 1200 furnace according to BS/EN/ISO 18122:2015 and BS/ISO 1171:2010, for the biomass samples and coal sample, respectively. The fuel ashes were ground to $<75 \mu\text{m}$ in an agate mortar and stored in sealed glass containers. Due to the difference in the ash contents of the fuels, the ash blends were prepared according to the ash contents of the pure fuels and the chosen biomass blending ratio. For instance, the blend consisting of BC 60 wt% and SCG 40 wt%, namely BC60:SCG40, has an actual ash ratio of 91.1 wt% BC ash (prepared at 815 °C) and 8.9 wt% SCG ash (prepared at 550 °C) because the ash contents of BC and SCG are 7.99 wt% and 1.19 wt%, respectively. Blends of the BC ash with the WS ash at the same biomass blending ratios (i.e. 40, 60, and 80 wt% WS) were prepared for comparison purposes. All the ash blends were submitted to vibrating mixing in an electromagnetic shaker until they reached uniformity and kept in sealed glass containers. Table 3 shows the mass proportions used to prepare the ash blends samples based on the ash contents of the fuels.

2.3. Ash fusibility temperatures (AFT) studies

The ash behaviours from sintering/shrinkage to melting of pure fuel ashes and their blends were characterised by the determined ash

fusibility temperatures. AFT studies have shown to be adequate to predict initial deformation temperature (DT), softening temperature (ST), hemispherical temperature (HT), and flow temperature (FT) [43-47]. Cylindrical ash pellets were prepared using 100 mg of the ash samples and their blends in a 5 mm Specac evacuable die set. An Instron 3369 tensometer system was used to produce consistent ash pellets under a maximum compression pressure of 5000 psi with a holding time of 60 s. Each ash pellet was stored in a separate glass container. This ash pelleting method has shown improved results in the identification of DT, reduced error, and enhanced pellet height change identification [48].

The AFT measurements were performed according to BS ISO 540:2008 using a Carbolite CAF G5 fusibility furnace. The ash pellets were heated at 7 °C/min to 1580 °C under oxidising conditions (CO₂) at 1 l/min at ambient temperature and pressure (ATAP). Changes in the pellets shape were detected by a thermal digital camera and recorded every 5 °C. The experiments for each ash blend under the same experimental conditions were carried out at least twice to verify repeatability and a third experiment was carried out if the results differed by more than 2 %. Based on the recorded images, four characteristic temperatures namely DT, ST, HT, and FT were determined according to the changes in the cylindrical ash pellets.

Initially, the analysis of the recorded images to determine the fusion temperatures was carried out by manual method through the CAF test software, which allowed the placing of a grid over the sample under study in the image. A vector-based image processing application was later devised in MATLAB to analyse the recorded images and to determine the fusibility temperatures. The vector-based image processing application allowed the tracking of the changes in the sample shape by isolating the region of interest in the image. It provided a greater possibility to zoom-in and implemented a finer grid compared to the manual method provided by the CAF software. In addition, the analysis of the recorded images using the vector-based image processing application facilitated the comparison of changes among the samples in the same image. Fig. 2 shows the improvement in the tracking of changes of the ash blends cylinder samples using the vector-based image processing application.

2.4. Bubbling fluidised bed combustion system

Fig. 3 shows the experimental facilities with a 30 kW_{th} bubbling fluidised bed (BFB) combustion system. The detailed description of the BFB combustor and auxiliaries (fluidisation air fan, gas sampling and analysis, etc.) was provided in the previous studies from the authors [49] and only a brief introduction of the experimental procedure is presented below.

The experimental set-up in Fig. 3 was used for conducting the combustion experiments of the coal and biomass blends. The combustion air was used as fluidisation air and delivered to the nozzle-type air distributor plate by a centrifugal fan. The airflow rate was controlled using a ball valve arranged in the air pipe downstream from the fan and monitored by a variable area volumetric air flow meter. Prior to the start of the fuel feeding, the silica sand bed in the BFB combustor was pre-heated using two semi-cylindrical radiant heaters. Upon attaining the bed temperature of 600 °C, the fuel feeder was switched on to start the fuel feeding. The fuel feeding rate was controlled by the feeder motor inverter frequency according to the screw feeder calibration results. The differential pressure across the dense bed region and temperatures of the BFB combustor were continuously measured using a pressure differential transducer and six sheathed K-type thermocouples, respectively [49].

2.5. Operating conditions and characterisation methods

In all the experiments, the same amount of sand particles of approximately 6.00 kg was used with a static bed height of approximately 200 mm as the inert bed material in the BFB combustor. The fuel

Table 2
Chemical composition of the bed material (by XRF).

	Silica sand
SiO ₂	96.67
P ₂ O ₅	<0.01
Fe ₂ O ₃	2.4
Al ₂ O ₃	0.33
CaO	0.01
MgO	<0.01
Na ₂ O	0.03
K ₂ O	0.01
TiO ₂	0.03



Fig. 1. SCG pellets manufacturing progression, (a) Raw SCG as received (moisture content greater than 60 wt%), (b) Dried SCG (moisture content \sim 15 wt%), and (c) manufactured SCG pellets.

Table 3

Proportions of ash from bituminous coal (BC), spent coffee grounds (SCG), and wheat straw (WS) in the ash blends prepared for Ash Fusibility Tests.

Fuel blend Designation	Biomass ratio (wt%)	Mass proportions of ash in the blend (wt%)		
		BC	SCG	WS
BC60:SCG40	40	91.1	8.9	–
BC40:SCG60	60	82.1	17.9	–
BC20:SCG80	80	63.0	37.0	–
BC60:WS40	40	65.7	–	34.3
BC40:WS60	60	46.0	–	54.0
BC20:WS80	80	24.2	–	75.8

feeding was occasionally finely adjusted during the tests to maintain the pre-set operating temperature. The volumetric flow rate of the fluidising air was maintained at the same value of 38.4 m³/h at ambient temperature and pressure (ATAP) throughout the test period. Due to the operational challenges caused by the interest to investigate the agglomeration tendency at high operating temperatures, the excess air levels of the combustion tests were not optimised in this study. The flue gas leaving the BFB combustor via the cyclone was continuously sampled and conditioned by means of water condensation traps and particulate filters. The concentrations of O₂, CO₂, and CO in the cleaned gas sample were measured by an ABB Easy line continuous gas analyser (EL3020), whereas the NO_x concentration was measured by a Horiba

chemiluminescent NO_x analyser (VA-3000). The temperature, pressure drop, and gas concentrations were continuously measured and recorded using a data acquisition system (DT80 DataTaker). At the end of each experiment the reactor was cooled down before the bed material was discharged from the bottom of the BFB test rig, followed by visual inspection for the signs of agglomeration and the presence of agglomerates. The remaining fuel in the hopper was weighed to double-check the fuel consumption rate and perform the determination of gaseous emissions (CO₂, CO, and NO_x) on an energy basis by the analysis of collected data from the gas analysers. Samples of bed materials and particles in the cyclone particulate container (mainly ash) were collected and analysed by Scanning Electron Microscopy with dispersive X-ray microanalysis (SEM-EDX) and X-ray fluorescence (XRF) techniques, and ASTM D7348 Standard Test Method for Loss on Ignition (LOI) of Solid Combustion Residues according to the methodology implemented in previous published work of the authors [49].

3. Results and discussion

3.1. Ash fusibility temperatures (AFT) studies

3.1.1. Ash fusibility temperatures of pure fuels

AFT studies using the ashes from BC, SCG, and WS were conducted and their fusibility temperatures are shown in Fig. 4. The different ash fusibility behaviours among the fuels are attributed to the variation in

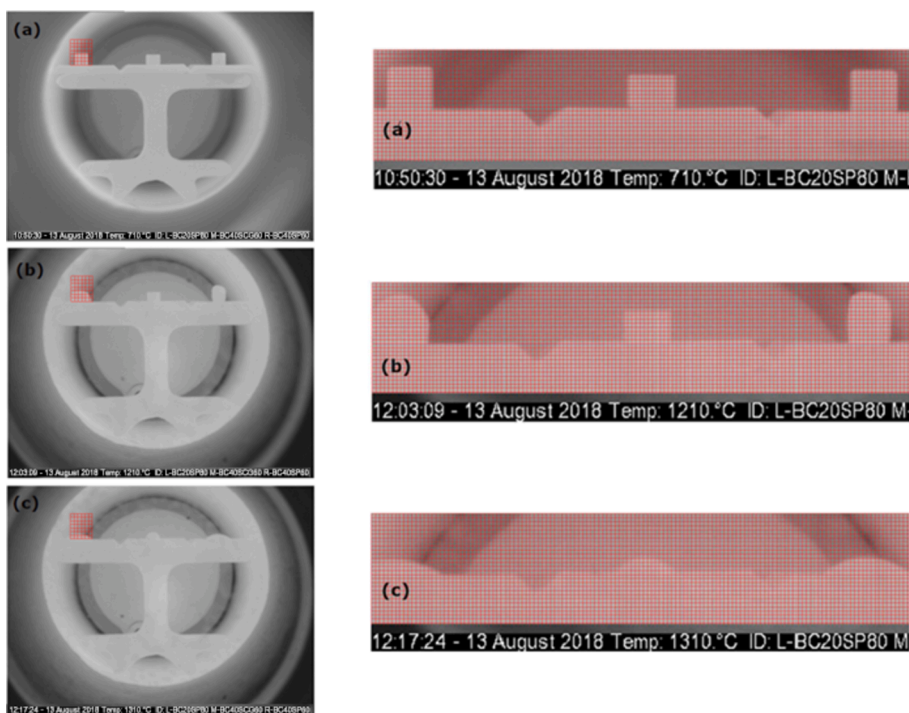


Fig. 2. Comparison of the manual method using CAF software (left) and the vector-based image processing application devised in this study (right) to perform the AFT analysis, (a) at 710 °C, (b) at 1210 °C, and (c) 1310 °C.

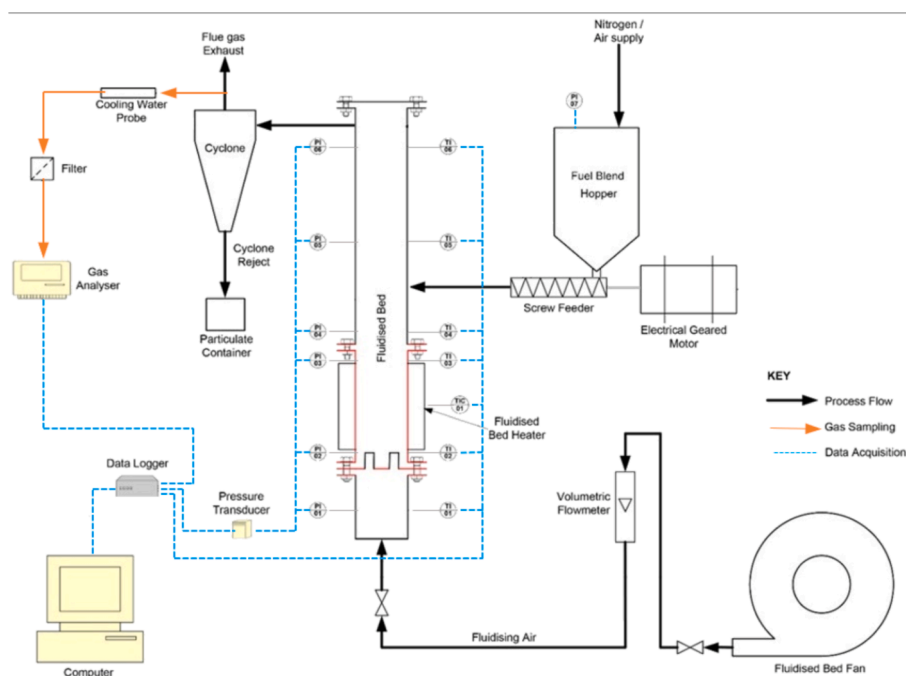


Fig. 3. Schematic diagram of the pilot-scale BFB combustion system [50].

their ash compositions. Lower AFT values and a broader range were observed for the WS ash and SCG ash in comparison to the BC ash. It is widely accepted that higher contents of SiO_2 and Al_2O_3 , and lower contents of CaO , Fe_2O_3 , MgO and K_2O in coal ash are responsible for its high AFT values [47]. Acidic oxides such as Al_2O_3 and SiO_2 are responsible for high AFT values of coal ash because these oxides with high ionic potentials are prone to combine with oxygen to form polymers, causing the AFT values to increase [28,32,43].

Compared to the WS ash, the SCG ash showed higher AFT values with only slightly lower than those for the BC ash. These findings are consistent with those of Wei et al. [51], who also reported high AFT values for their SCG ash. The high AFT values of the SCG ash are attributed to the low SiO_2 content in the SCG ash, despite of the high K_2O and P_2O_5 contents in the ash, accounting for more than 56 wt% of the total SCG ash. Numerous studies have reported that a high P_2O_5 content in ash can lead to low AFT values due to the development of low melting

phases in the ash [52]. Furthermore, high contents of SiO_2 and K_2O in ash have been linked to low AFT values and ash sintering issues [53]. Nevertheless, the formation of potassium silicates with low AFT values has been reported to be limited by the availability of silicon in the fuel ash [53].

The WS ash showed considerably lower DT and ST values compared to the SCG ash and BC ash. This is attributed to the high SiO_2 and K_2O contents in the WS ash. Moreover, the difference between DT and ST for the WS ash was only 75 °C where a difference of 97 °C between DT and ST was found for the SCG ash. A smaller difference between DT and ST has been linked to sharp changes in the viscosity of the biomass ash with the temperature once DT has been reached [30]. The SCG ash showed higher ST, HT, and FT values than the ash of WS used in this study and other biomass resources reported in the literature [54-56]. This is mainly attributed to the relatively high CaO and MgO contents and low SiO_2 content in the SCG ash.

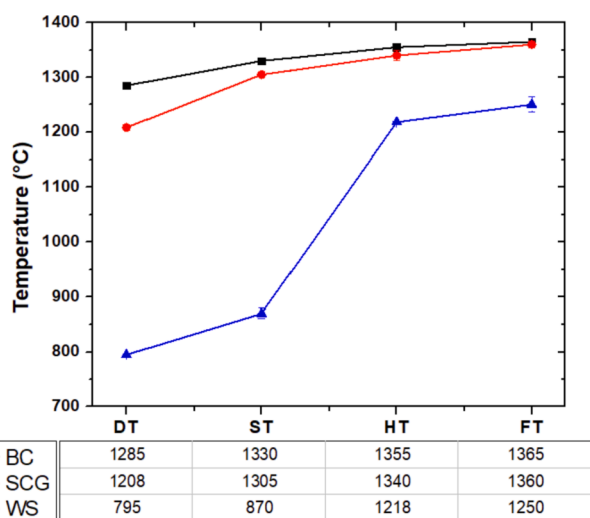


Fig. 4. Ash fusion temperatures (deformation-DT, sphere-ST, hemisphere-HT, and flow-FT) for bituminous coal (BC), wheat straw (WS), and spent coffee grounds (SCG).

3.1.2. Ash fusibility of bituminous coal and wheat straw blends

Fig. 5 shows the AFT values of the BC ash blended with the WS ash at the corresponding fuel blending ratios of 40, 60, and 80 wt%. As mentioned in Section 2.2, the actual ash blends were prepared according to the ash contents of the fuels and the stated blending ratio of the biomass fuel in the biomass-coal mixture. The increase in the blending ratio of WS in the BC-WS blends gradually shifted the fusibility temperatures of the ash blends from the values of the BC ash to those of the WS ash. In addition, the AFT values of the ash blends were always lower than those of the BC ash and greatly differed from the fusibility temperatures of the pure fuels. This can be attributed to the significant changes in the composition of the ash resulting from the addition of WS to BC in the ash blends (see S1 and S2 in the supplementary material). The increase in the blending ratio of WS in the BC-WS blends reduced the Al_2O_3 and Fe_2O_3 contents of the ash blends. The coal ash contains significant levels of these two compounds (see Table 1), which have high fusibility temperatures under oxidising conditions [57]. Further, the SiO_2 , K_2O and Cl contents in the ash blends increased with the WS blending ratio due to the higher levels of these compounds in the WS ash than the coal ash (see Table 1).

The addition of the WS ash to the BC ash lowered the AFT values of all ash blends and this was true even at the lowest blending ratio (40 wt

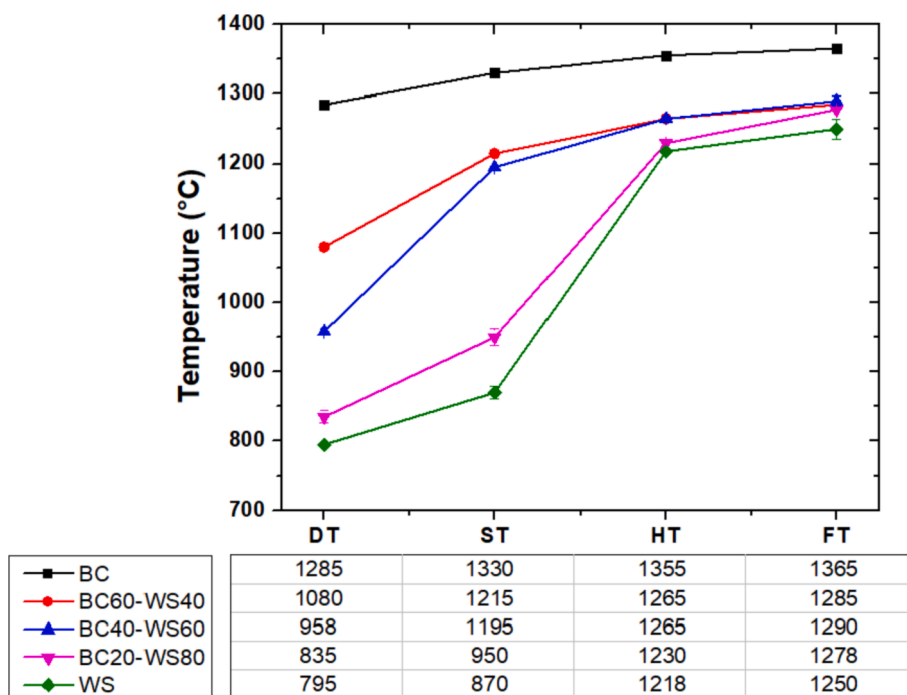


Fig. 5. Ash fusibility temperatures (deformation-DT, sphere-ST, hemisphere-HT, and flow-FT) of bituminous coal (BC) ash blended with wheat straw (WS) ash.

% WS in the BC-WS blend) investigated in this study. This is attributed to the significant change in the ash blends composition as a result of the comparable ash content in WS to that of the coal and the higher contents of SiO₂, K₂O, and Cl in the WS ash. The coexistence of SiO₂ and K₂O, and Cl has been reported as one of the factors responsible for forming low-melting K-silicates, which decrease the AFT values [30,58] or lead to sintering and agglomeration of the bed material in fluidised beds [53].

3.1.3. Ash fusibility of bituminous coal and spent coffee grounds blends

Fig. 6 shows the AFT values of the BC ash blended with the SCG ash with the corresponding fuel blending ratios of 40, 60, and 80 wt%. The

contents of SiO₂, Fe₂O₃, and Al₂O₃ in the ash blends decreased with the SCG blending ratio. This is due to the much lower contents of these compounds in the SCG ash than in the coal ash (see Table 1, S3 and S4 in the supplementary material). An increase in the blending ratio of SCG in the BC-SCG blends increases the K₂O, CaO, MgO, and P₂O₅ contents of the ash blends. This is due to the fact that these compounds were found to be rich in the SCG ash (Table 1). High levels of CaO, MgO, and P₂O₅ in ash lead to high fusibility temperatures under oxidising conditions [55,56,59]. Furthermore, the SiO₂ to Al₂O₃ ratio in the BC-SCG blends remained constant with a value of 1.22 regardless the SCG blending ratio. This is due to the fact that the SiO₂ and Al₂O₃ contents in the ash

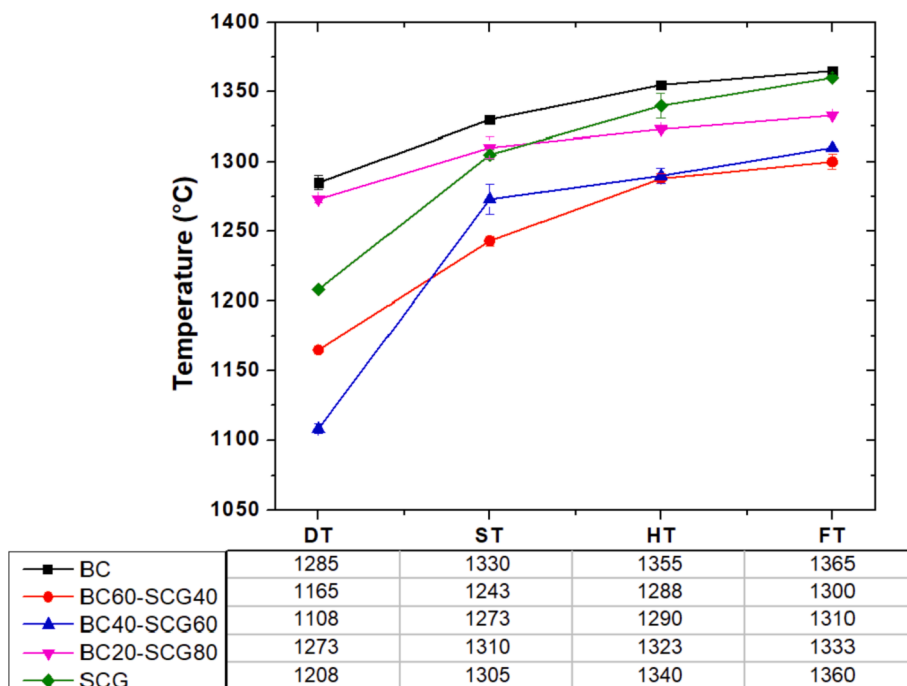


Fig. 6. Ash fusion temperatures (deformation-DT, sphere-ST, hemisphere-HT, and flow-FT) of bituminous coal (BC) ash blended with spent coffee grounds (SCG) ash.

blends come from BC ash only. Low SiO_2 to Al_2O_3 ratio values in ash have been linked to high AFT values [28,59].

Compared to the blends of the BC ash and the WS ash, the AFT values of the BC ash and the SCG ash blends did not show a constant decreasing trend against the blending ratio. This is mainly attributed to the reducing availability of SiO_2 in the BC-SCG ash blends when the SCG blending ratio increases. Similar results were reported by Teixeira et al. [53] during AFT experiments using blends of coal and olive cake which had negligible SiO_2 content in the ash. Furthermore, the changes in the AFT values for the BC-SCG blends were not as significant as for the BC-WS blends despite the high content of K_2O in the SCG ash. This is attributed to the low ash content of the SCG compared to the coal used in this study (see Table 1). The changes in the DT values for the blends of the BC ash with either the WS ash or SCG ash cannot be predicted by a simple linear correlation of the ash ratio in the blends as shown in Fig. 7.

The DT values of the BC-SCG ash blends initially decreased below the DT values of the individual BC and SCG ashes for the blending ratios corresponding to 40 and 60 wt% SCG, then an increase in the DT value corresponding to the blending ratio of 80 wt% SCG was observed. This increase in the DT value was confirmed by several repeating fusibility

tests using the same ash blending ratio (80 wt% SCG in the BC-SCG blend). The error bars shown in Fig. 7 were calculated from the results of the repeating fusibility tests at each of the investigated blending ratios. This can be explained by the markedly different chemical and mineral composition of fuels' ash and complex interactions due to the mineral evolution with the temperature increase. The increase in the DT value for BC blended with 80 wt% SCG is attributed to interactions among the ashes from the pure fuels leading to high melting temperatures compounds. Similar findings were reported as a result of the formation of high-melting temperature mullite in larger amounts than compared to the original coal ash during AFT studies of blends of ash from coal and biomass by Ma et al. [32], Li et al. [35], and Li et al. [60]. This behaviour has also been reported as typical eutectic melting during ash fusibility experiments of coal blends [61]. In addition, Song et al. [62] and Zhu et al. [58] reported the increase in the formation of high melting Mg- or Ca-silicates as well as Mg- and Ca-Al-silicates during AFT experiments of coal ash blends and blends of coal and biomass, respectively, concluding that higher CaO and MgO contents in the fuel ash could increase the AFT values and reduce the risk of slagging. Li et al. [60] attributed the increase in the formation of high melting temperatures compounds to the substitution of K by Ca in semi-molten aluminosilicates. These results suggest that the fusibility behaviour of the ash blends used in this study is not additive and greatly differs from the behaviour of the individual fuel ashes. Similar findings have been reported by Li et al. [35], Wang et al. [43], Li et al. [57], Shen et al. [61], and Link et al. [63].

The ternary diagram proposed by Link et al. [63] was used to illustrate the changes in the ash blends composition. This diagram uses the total content of alkali oxides $\text{Na}_2\text{O} + \text{K}_2\text{O}$, alkaline earth oxides $\text{CaO} + \text{MgO}$, and acidic and intermediate oxides $\text{SiO}_2 + \text{Al}_2\text{O}_3 + \text{Fe}_2\text{O}_3 + \text{P}_2\text{O}_5$ in each corner. The contribution of other oxides and Cl to the average composition was neglected. The analysis consisted of the calculated ash blend composition according to the blending ratio (see S1, S2, S3, and S4 in the supplementary material). Fig. 8 shows the change in the ash composition of the BC ash blended with either the WS ash or SCG ash. Despite the low ash content of SCG, the blends of the BC ash with the SCG ash showed a broad change in their composition. This is attributed to the increasing content of CaO, K_2O , and MgO in the blends when the SCG ash blending ratio increases. A high content of CaO favours the formation of Ca-Silicates or Ca-K-Silicates with high melting temperatures instead of K-Silicates with lower melting temperatures [46,47,53]. In contrast, the blends of the BC ash with the WS ash with high SiO_2 and K_2O contents showed a narrow change of the compounds in the ash blends. High contents of SiO_2 and K_2O in the fuel ash have been linked to

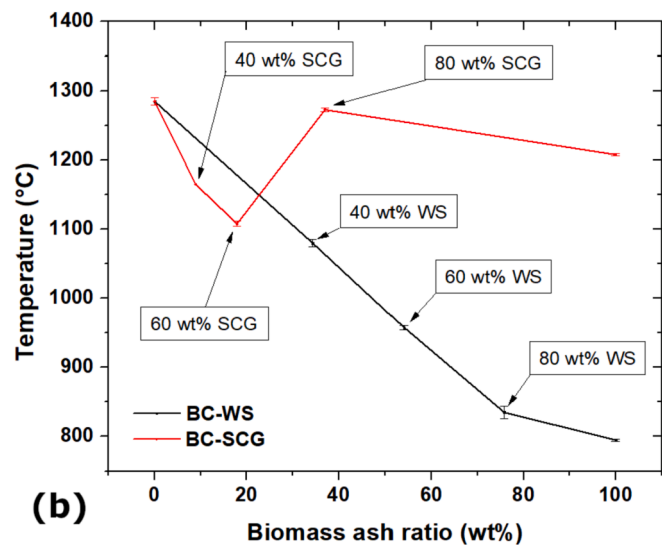
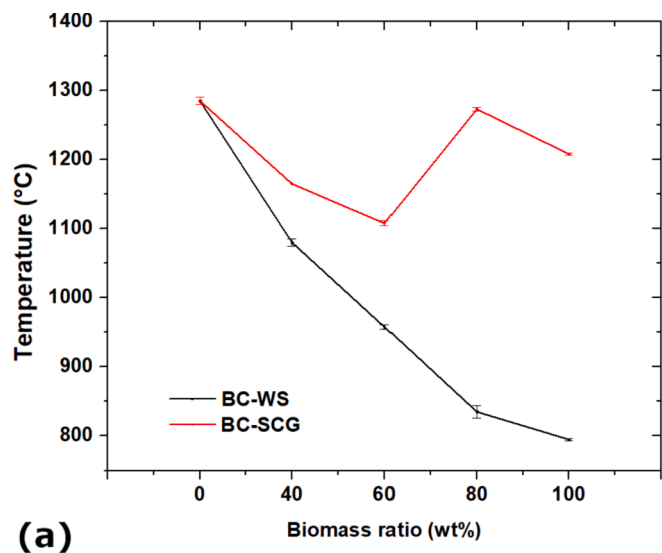


Fig. 7. Comparison of deformation temperature (DT) for the bituminous coal (BC) ash blended with the spent coffee grounds (SCG) ash and the wheat straw (WS) ash. (a) DT vs biomass ratio, (b) DT vs ash ratio.

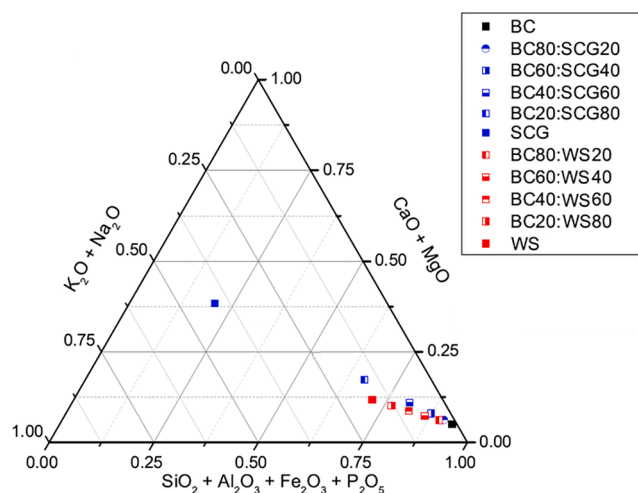


Fig. 8. Ternary diagram of bituminous coal (BC) ash blended with spent coffee grounds (SCG) and wheat straw (WS).

decreasing AFT values of the ash blends. Zhu et al. [58] reported similar findings during AFT experiments using blends of corn straw and sawdust, and further studies of the effects of SiO₂, K₂O, CaO, and MgO as additives.

3.2. Co-combustion experiments in a fluidised bed combustor

3.2.1. CO, combustion performance, and NO_x emissions.

Fig. 9 illustrates the CO emissions when blends of BC with SCG at the blending ratio of 40 wt% were used in comparison to pure BC and blends of BC with WS at the same blending ratio. The blends used in this study did not show a significant difference in terms of the CO emissions under the experimental conditions compared to pure bituminous coal.

The combustion performance was determined by the loss of efficiency due to unburnt carbon (UBC) in ash and CO emissions according to the methodology provided in the previous studies from the authors on this combustor [49]. Fig. 10 shows the efficiency loss due to unburnt carbon (UBC) and CO emissions when BC blended with SCG at 40 wt% was used in comparison to pure BC and BC blended with WS at the same blending ratio. A reduced loss of efficiency was achieved when BC was blended with either WS or SCG compared to pure BC. Furthermore, BC blended with SCG showed a lower loss of efficiency compared to when BC was blended with WS. This is mainly attributed to the lower ash content of SCG compared to the other fuels used in this study. Biomass addition to coal combustion results in higher combustion efficiencies due to higher volatile matter content of biomass compared to coal. These results show that the gain in combustion efficiency is mainly attributed to the reduction in UBC. Several studies on co-combustion of coal and biomass in fluidised beds have reported similar trends [64].

The effect of blending BC with biomass at 40 %wt on NO_x emissions is illustrated in Fig. 11. The NO_x emissions were higher when BC was blended with SCG compared to when BC was blended with WS. In fact, the NO_x emissions when BC was blended with SCG showed to be similar to the emissions from pure BC. It is well known that NO_x levels are mainly determined by the nitrogen content in the solid fuels [49,65]. Despite the higher nitrogen content in SCG than BC and WS (by 33 % and 214 %, respectively, see Table 1), the combustion of BC blended with SCG did not show an obvious change in NO_x emissions compared to the combustion of pure BC. This can be explained by the release of fuel nitrogen mainly as ammonia (NH₃) with biomass combustion [66]. The conversion ratio of NH₃ to NO is lower in comparison to that of HCN, which is the main product of coal fuel nitrogen, to NO [67,68]. Furthermore, the rapid release of biomass volatiles leads to high concentrations of

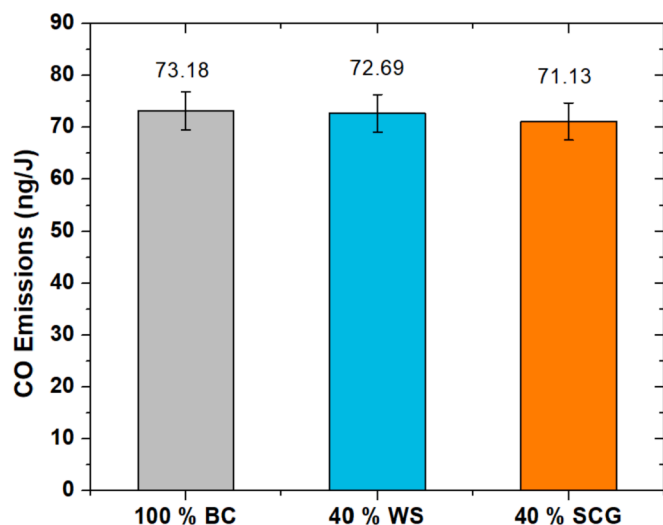


Fig. 9. CO emissions, bituminous coal (BC), BC with spent coffee grounds (SCG) blended at 40 wt%, and BC with wheat straw (WS) blended at 40 wt%.

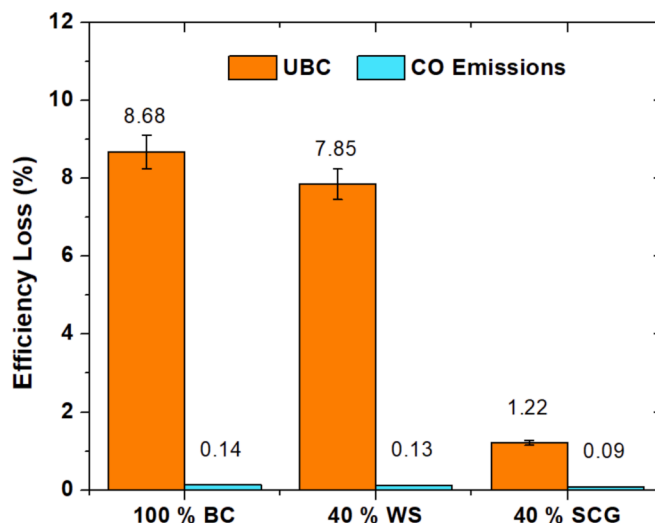


Fig. 10. Comparison of bituminous coal (BC), BC blended with spent coffee grounds (SCG) at 40 wt%, and BC blended with wheat straw (WS) at 40 wt% in terms of loss of efficiency due to unburnt carbon (UBC) and CO emissions.

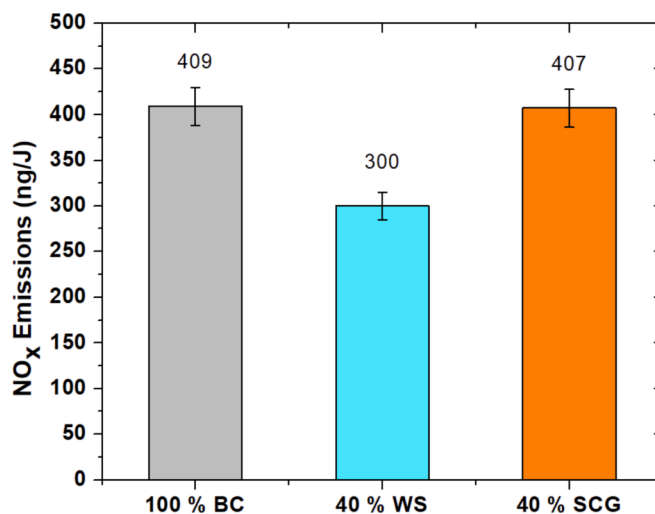


Fig. 11. NO_x emissions, bituminous coal (BC), BC blended with spent coffee grounds (SCG) at 40 wt%, and BC blended with wheat straw (WS) at 40 wt%.

hydrocarbon radicals in the combustion zone, promoting the reduction of NO (see R1-R3) during the co-combustion of coal and biomass. In addition, higher levels of volatile matter with coal-biomass blends produce high concentrations of CO at the early stage of combustion, while CO can react with NO to produce N₂ (see R4) [69-71], which can be catalysed by inorganic impurities and even the char at high temperatures [69]. These results are consistent with the findings of Limousy et al. [14], Byul et al. [27], Allesina et al. [72], and Jeguirim et al. [26,41], and confirm the potential of SCG to be combusted in blends with coal without increasing harmful NO_x emissions.



3.2.2. Effect of biomass blending on agglomeration tendency

In contrast to the agglomerates found when BC was blended with WS

as shown in Fig. 12, with detailed characterisation being provided in the previous studies from the authors on this BFB combustor [49], the visual inspection of the used bed material when BC was blended with SCG did not show the existence of agglomerates. Despite the operation time with the combustion test of BC blended with SCG at 40 wt% was extended to 20 h, i.e. doubling the operation time that was carried out with the combustion test of BC blended with WS at 40 wt%, there were no agglomerates bigger than the top size of the silica sand bed materials found with the co-combustion of the BC-SCG blend.

3.3. Characterisation of used bed material and cyclone ash

3.3.1. Scanning Electron Microscopy coupled with energy disperse X-ray spectroscopy (SEM-EDS) of the used bed material

Fig. 13 shows the EDX mapping analysis of the used bed particles after the combustion of BC blended with SCG at 40 wt%. The distribution of Al, K, Fe, Ca, Si, Mg, and O across the surface of the used bed particle samples was identified as present. The intensity of the colour across a particular area indicates the extent of the element in that region. The results from EDX mapping analysis clearly showed the existence of cracks in the used bed particles. The presence of cracks has been linked to mechanical and chemical stress, which can lead to attrition and fragmentation of the bed particles [73]. Al, K, and Fe were the dominant elements in the cracks, with a lesser intense presence of Ca and Mg. These results agree with findings from the AFT studies in section 3.1.3 in terms of K, Ca, and Mg as the most active elements in the SCG ash. The distribution of O across the used bed material (Fig. 13) can be considered an indication of the presence of studied elements in their oxidised forms.

Further analysis of the used bed particles based on EDX spot technique shown in Fig. 14 revealed the existence of a thin coating layer



Fig. 12. Sample of agglomerates collected from the combustion of bituminous coal (BC) blended with wheat straw pellets (WS) at 40 wt% after 10 h of operation using silica sand as bed material (scale in cm). Picture from published work of the authors [49].

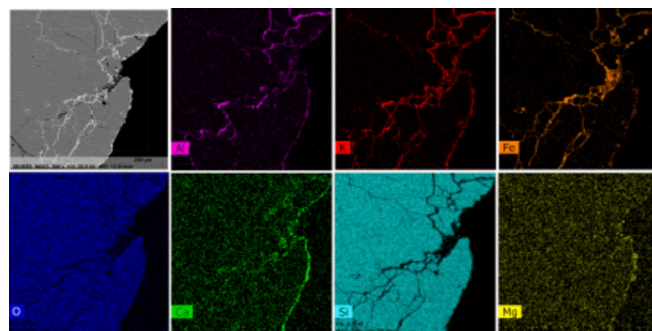


Fig. 13. EDX elemental mapping of Garside 14/25 bed material samples from combustion of BC blended with SCG at 40 wt% after 20 h of operation.

(<10 μm). This coating layer consisted of a two-layer structure with substantial contents of Si, K, Ca, and Fe in the innermost layer, indicating the role of an adhesive $\text{K}_2\text{O}-\text{CaO}-\text{SiO}_2$ system in the formation of the primary coating layer on the used bed particles. Fe found in this layer could be mainly derived from the fuel blend (see Table 1). Nevertheless, the precipitation of Fe to the surface of the silica sand particles was reported by Afilaka [50], who conducted coal combustion experiments

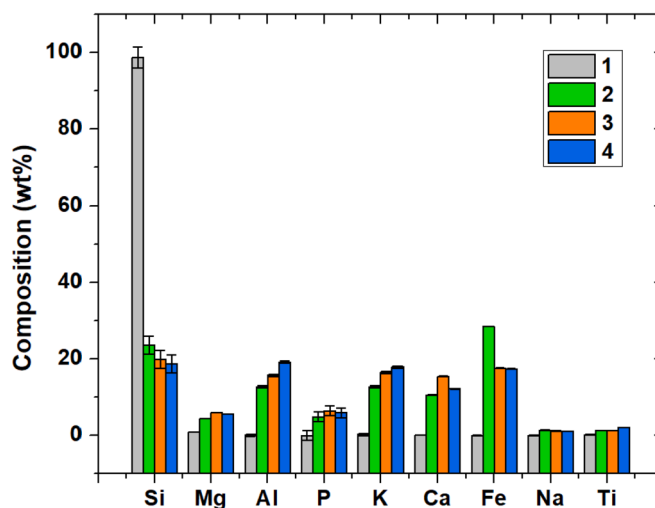
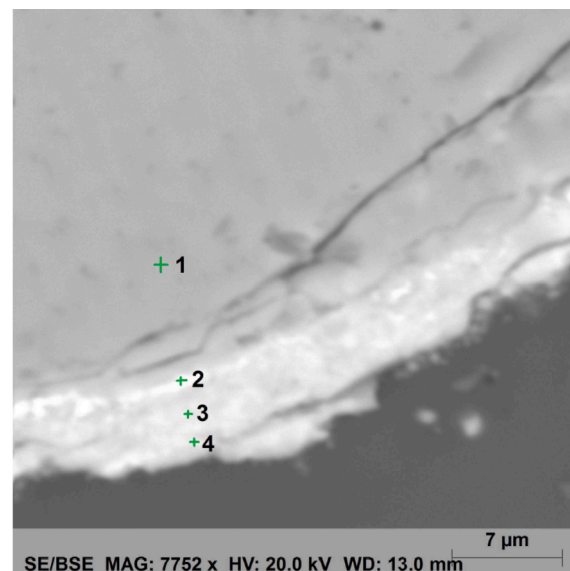
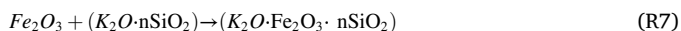
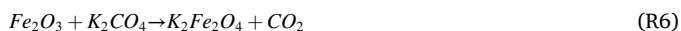
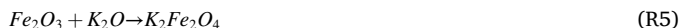


Fig. 14. EDX elemental spot analysis of Garside 14/25 bed material sample from the combustion of BC blended with SCG at 40 wt% after 20 h of operation.

in the BFB combustor using the same silica sand bed material as this study. Fe on the sand particle surface could further react with the potassium compounds to form the coating layer (see R5-R7). The outermost layer showed an increasing trend in the content of K. The contents of Al, Ca, Fe, and Mg also showed an increasing trend in the outermost layer. These elements are known for their high ash melting temperatures. This explains the reduced agglomeration tendency when the blend of BC with 40 wt% SCG was combusted.



3.3.2. X-Ray fluorescence (XRF) analysis of cyclone ash

Further XRF analyses of the cyclone ash from the combustion of BC blended with SCG at 40 wt% were performed to investigate the effect of the biomass blending on the cyclone ash elemental composition. For comparison purpose, the cyclone ashes from the combustion of BC in pure and BC blended with WS at 40 wt% were also analysed. The results shown in Fig. 15 reveal an increase in K, Mg, Ca, and P contents in the cyclone ash when coal/biomass blends were combusted in comparison to pure BC. Compared to the cyclone ash of BC blended with WS, the cyclone ash of BC blended with SCG had higher contents of Fe, Al, P, and Mg and a reduction in the content of Si. These results confirm earlier findings from the AFT studies in Section 3.1.3 about K, Mg, and Ca as the most active elements along with the reduced Si content when BC was blended with SCG in comparison to pure BC.

4. Conclusions

The main conclusions of the present study are as follows:

1. SCG was shown to have the potential to be an excellent fuel due to its relatively high heating value, high volatile matter content, low ash content, and higher ash fusibility temperatures than those of the WS ash and other biomass ashes reported in the literature (e.g. cotton stalk, bagasse, waste bamboo, and rice straw), with the sphere temperature (ST), hemisphere temperature (HT), and flow temperature (FT) values only slightly lower than those for the BC ash despite the high K_2O content in the SCG ash.
2. The ash blend corresponding to 20 wt% coal – 80 wt% SCG was found to have a much higher deformation temperature (DT) than that of the SCG ash, with the value only slightly lower than that for the BC ash. However, the ash blends corresponding to 40 wt% coal – 60 wt% SCG and 60 wt% coal – 40 wt% SCG were found to have lower DT values than those of the SCG ash.
3. The addition of SCG to BC led to a lower combustion efficiency loss resulted from the unburned carbon in ash in comparison to the combustion of pure BC or BC-WS blends. This suggests SCG has the potential to improve the efficiency of coal combustion under co-combustion conditions.
4. Despite of the fact that SCG has a higher content of fuel nitrogen than the BC, similar NO_x emissions were found for the co-combustion of 60 wt% BC and 40 wt% SCG and the combustion of pure BC under the investigated conditions in this study. This indicates SCG can be co-combusted with coal to avoid potential higher NO_x emissions when combusted in pure form.
5. The detailed analysis of the used bed material and cyclone ash by means of XRF and SEM/EDX provided further evidence about the reduced tendency of the bed material agglomeration during the co-combustion of coal with SCG, unlike the combustion of coal with WS.

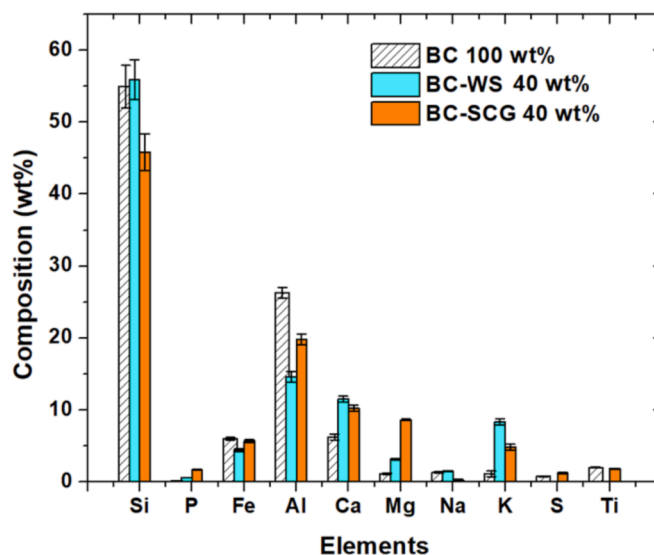


Fig. 15. Elemental composition (XRF) of cyclone ash from the combustion of BC blended with SCG pellets at 40 wt% and BC blended with wheat straw (WS) pellets at 40 wt% (Bituminous coal (BC) at 100 wt% was included for comparison purpose).

CRediT authorship contribution statement

Eduardo Garcia: Investigation, Formal analysis, Validation, Conceptualization, Methodology, Writing – original draft. **Manuel F. Mejía:** Methodology, Software, Formal analysis, Visualization. **Hao Liu:** Conceptualization, Methodology, Writing – review & editing, Supervision, Project administration.

Declaration of Competing Interest

The authors declare that they have no known competing financial interests or personal relationships that could have appeared to influence the work reported in this paper.

Acknowledgements

The research was supported by a Doctoral Research Fellowship from the Administrative.

Department of Science, Technology, and Innovation of Colombia (COLCIENCIAS), Newton-Caldas Fund – Conv. No.-679-2014, and COLFUTURO.

The authors would also like to thank British Sugar (<https://www.britishsugar.co.uk/>), and Agripellets (<https://www.agripellets.com/>) for the support on the tested coal and biomass fuel; respectively. The authors thank the Nanoscale and Microscale Research Centre (nmRC) (<https://www.nottingham.ac.uk/NMRC/>) for providing access to instrumentation.

Appendix A. Supplementary data

Supplementary data to this article can be found online at <https://doi.org/10.1016/j.fuel.2022.125008>.

References

- [1] IEA, Global Energy & CO₂ Status Report, 2019. <https://www.iea.org/reports/global-energy-co2-status-report-2019>.
- [2] IEA, Global Energy Review 2019, 2020. <https://www.iea.org/reports/global-energy-review-2019>.
- [3] World Energy Council, World Energy Resources, Coal, 2016.
- [4] IEA, Key Coal Trends, 2016. <https://euagenda.eu/upload/publications/untitled-69166-ea.pdf>.

- [5] Larionov KB, Mishakov IV, Slyusarskiy KV, Tsubulskiy SA, Tabakaev RB, Bauman YI, et al. Combustion of bituminous coal and semicoke with copper salts. *Fuel Process Technol* 2021;213:106706. <https://doi.org/10.1016/j.fuproc.2020.106706>.
- [6] Sahu SG, Chakraborty N, Sarkar P. Coal-biomass co-combustion: An overview. *Renew Sustain Energy Rev* 2014;39:575–86. <https://doi.org/10.1016/j.rser.2014.07.106>.
- [7] Zhou C, Liu G, Wang X, Qi C. Co-combustion of bituminous coal and biomass fuel blends: Thermochemical characterization, potential utilization and environmental advantage. *Bioresour Technol* 2016;218:418–27. <https://doi.org/10.1016/j.biortech.2016.06.134>.
- [8] Wladyslaw M. Co-Combustion of Pulverized Coal and Biomass in Fluidized Bed of Furnace. *J Energy Resour Technol* 2017;139:062204. <https://doi.org/10.1115/1.4036958>.
- [9] Hupa M. Ash-related issues in fluidized-bed combustion of biomasses: Recent research highlights. *Energy & Fuels* 2012;26:4–14. <https://doi.org/10.1021/ef201169k>.
- [10] IRENA, Biomass Co-firing - Technology brief, 2013. <https://www.irena.org/publications/2013/Jan/Biomass-co-firing>.
- [11] Campos-Vega R, Loarca-Piña G, Vergara-Castañeda H, Oomah BD. Spent coffee grounds: A review on current research and future prospects. *Trends Food Sci Technol* 2015;45:24–36. <https://doi.org/10.1016/j.tifs.2015.04.012>.
- [12] Murthy PS, Madhava Naidu M. Sustainable management of coffee industry by-products and value addition - A review. *Resour Conserv Recycl* 2012;66:45–58. <https://doi.org/10.1016/j.resconrec.2012.06.005>.
- [13] Mata TM, Martins AA, Caetano NS. Bio-refinery approach for spent coffee grounds valorization. *Bioresour Technol* 2018;247:1077–84. <https://doi.org/10.1016/j.biortech.2017.09.106>.
- [14] Limousy L, Jeguirim M, Dutournié P, Kraiem N, Lajili M, Said R. Gaseous products and particulate matter emissions of biomass residential boiler fired with spent coffee grounds pellets. *Fuels* 2013;107:323–9. <https://doi.org/10.1016/j.fuel.2012.10.019>.
- [15] Espuelas S, Marcelino S, Echeverría AM, Del Castillo JM, Seco A. Low energy spent coffee grounds briquetting with organic binders for biomass fuel manufacturing. *Fuel* 2020;278:118310. <https://doi.org/10.1016/j.fuel.2020.118310>.
- [16] Colantoni A, Paris E, Bianchini L, Ferri S, Marcantonio V, Carnevale M, et al. Spent coffee ground characterization, pelletization test and emissions assessment in the combustion process. *Sci Rep* 2021;11:1–14. <https://doi.org/10.1038/s41598-021-84772-y>.
- [17] Kim Y, Park T, Hong D. Heating and emission characteristics of briquettes developed from spent coffee grounds. *Environ Eng Res* 2021;27:210063. <https://doi.org/10.4491/eer.2021.063>.
- [18] Klingel T, Kremer JI, Gottstein V, De Rezende TR, Schwarz S, Lachenmeier DW. A review of coffee by-products including leaf, flower, cherry, husk, silver skin, and spent grounds as novel foods within the European Union. *Foods* 2020;9. <https://doi.org/10.3390/foods9050665>.
- [19] McNutt J, (Sophia) He Q. Spent coffee grounds: A review on current utilization. *J Ind Eng Chem* 2019;71:78–88. <https://doi.org/10.1016/j.jiec.2018.11.054>.
- [20] Chen YC, Zhou SY. Integrating spent coffee grounds and silver skin as biofuels using torrefaction. *Renew Energy* 2020;148:275–83. <https://doi.org/10.1016/j.renene.2019.12.005>.
- [21] Nosek R, Tun MM, Juchelkova D. Energy utilization of spent coffee grounds in the form of pellets. *Energies* 2020;13:1–8. <https://doi.org/10.3390/en13051235>.
- [22] Tun MM, Raclavská H, Juchelková D, Růžicková J, Šafář M, Štrbová K, et al. Spent coffee ground as renewable energy source: Evaluation of the drying processes. *J Environ Manage* 2020;275. <https://doi.org/10.1016/j.jenvman.2020.111204>.
- [23] Conesa JA, Sánchez NE, Garrido MA, Casas JC. Semivolatile and Volatile Compound Evolution during Pyrolysis and Combustion of Colombian Coffee Husk. *Energy Fuels* 2016;30:7827–33. <https://doi.org/10.1021/acs.energyfuels.6b00791>.
- [24] Mussatto SI, Machado EMS, Martins S, Teixeira JA. Production, Composition, and Application of Coffee and Its Industrial Residues. *Food Bioprocess Technol* 2011;4:661–72. <https://doi.org/10.1007/s11947-011-0565-z>.
- [25] Limousy L, Jeguirim M, Labbe S, Balay F, Fossard E. Performance and emissions characteristics of compressed spent coffee ground/wood chip logs in a residential stove. *Energy. Sustain Dev* 2015;28:52–9. <https://doi.org/10.1016/j.esd.2015.07.002>.
- [26] Jeguirim M, Limouisy L, Fossard E. Characterization of coffee residues pellets and their performance in a residential combustor. *Int J Green Energy* 2016;13:608–15.
- [27] Byul S, Young H, Jin J, Sung K. Characteristics of spent coffee ground as a fuel and combustion test in a small boiler (6.5 kW). *Renew Energy* 2017;113:1208–14. <https://doi.org/10.1016/j.renene.2017.06.092>.
- [28] Yan T, Bai J, Kong L, Bai Z, Li W, Xu J. Effect of SiO₂/Al₂O₃ on fusion behavior of coal ash at high temperature. *Fuel* 2017;193:275–83. <https://doi.org/10.1016/j.fuel.2016.12.073>.
- [29] Zhu Y, Hu J, Yang W, Zhang W, Zeng K, Yang H, et al. Ash Fusion Characteristics and Transformation Behaviors during Bamboo Combustion in Comparison with Straw and Poplar. *Energy Fuels* 2018;32:5244–51. <https://doi.org/10.1021/acs.energyfuels.8b00371>.
- [30] Deng L, Zhang T, Che D. Effect of water washing on fuel properties, pyrolysis and combustion characteristics, and ash fusibility of biomass. *Fuel Process Technol* 2013;106:712–20. <https://doi.org/10.1016/j.fuproc.2012.10.006>.
- [31] Dibdiakova J, Wang L, Li H. Characterization of Ashes from Pinus Sylvestris forest Biomass. *Energy Procedia* 2015;75:186–91. <https://doi.org/10.1016/j.egypro.2015.07.289>.
- [32] Ma X, Li F, Ma M, Fang Y. Investigation on Blended Ash Fusibility Characteristics of Biomass and Coal with High Silica-Alumina. *Energy Fuels* 2017;31:7941–51. <https://doi.org/10.1021/acs.energyfuels.7b01070>.
- [33] Lu G, Zhang K, Cheng F. The fusion characteristics of ashes from anthracite and biomass blends. *J Energy Inst* 2017;1–8. <https://doi.org/10.1016/j.joei.2017.05.001>.
- [34] Xing P, Darvell LI, Jones JM, Ma L, Pourkashanian M, Williams A. Experimental and theoretical methods for evaluating ash properties of pine and El Cerrejón coal used in co-firing. *Fuel* 2016;183:39–54. <https://doi.org/10.1016/j.fuel.2016.06.036>.
- [35] Li F, Xu M, Wang T, Fang Y, Ma M. An investigation on the fusibility characteristics of low-rank coals and biomass mixtures. *Fuel* 2015;158:884–90. <https://doi.org/10.1016/j.fuel.2015.06.010>.
- [36] De Fusco L, Defoort F, Rajczyk R, Jeanmart H, Blondeau J, Contino F. Ash Characterization of Four Residual Wood Fuels in a 100 kWth Circulating Fluidized Bed Reactor Including the Use of Kaolin and Halloysite Additives. *Energy Fuels* 2016;30:8304–15. <https://doi.org/10.1021/acs.energyfuels.6b01784>.
- [37] Morris JD, Daoud SS, Nimmo W. Agglomeration and the effect of process conditions on fluidized bed combustion of biomasses with olivine and silica sand as bed materials: Pilot-scale investigation. *Biomass Bioenergy* 2020;142:105806. <https://doi.org/10.1016/j.biombioe.2020.105806>.
- [38] Oakey J. Fuel Flexible Energy Generation: Solid, Liquid and Gaseous Fuels 2015. <https://doi.org/10.1016/C2014-0-01769-8>.
- [39] Whittaker C, Shield I. Factors affecting wood, energy grass and straw pellet durability - A review. *Renew Sustain Energy Rev* 2017;71:1–11. <https://doi.org/10.1016/j.rser.2016.12.119>.
- [40] Nunes LJR, Matias JCO, Catalão JPS. Mixed biomass pellets for thermal energy production: A review of combustion models. *Appl Energy* 2014;127:135–40. <https://doi.org/10.1016/j.apenergy.2014.04.042>.
- [41] Jeguirim M, Bikai J, Elmay Y, Limouisy L, Njeugna E. Thermal characterization and pyrolysis kinetics of tropical biomass feedstocks for energy recovery. *Energy. Sustain Dev* 2014;23:182–93. <https://doi.org/10.1016/j.esd.2014.09.009>.
- [42] Hu Q, Shao J, Yang H, Yao D, Wang X, Chen H. Effects of binders on the properties of bio-char pellets. *Appl Energy* 2015;157:508–16. <https://doi.org/10.1016/j.apenergy.2015.05.019>.
- [43] Wang D, Liang Q, Gong X, Liu H, Liu X. Influence of coal blending on ash fusion property and viscosity. *Fuel* 2017;189:15–22. <https://doi.org/10.1016/j.fuel.2016.10.050>.
- [44] Li J, Zhu M, Zhang Z, Zhang K, Shen G, Zhang D. Effect of coal blending and ashing temperature on ash sintering and fusion characteristics during combustion of Zhundong lignite. *Fuel* 2017;195:131–42. <https://doi.org/10.1016/j.fuel.2017.01.064>.
- [45] Niu Y, Tan H, Hui S. Ash-related issues during biomass combustion: Alkali-induced slagging, silicate melt-induced slagging (ash fusion), agglomeration, corrosion, ash utilization, and related countermeasures. *Prog Energy Combust Sci* 2016;52:1–61. <https://doi.org/10.1016/j.pecs.2015.09.003>.
- [46] Vassilev SV, Baxter D, Andersen LK, Vassileva CG. An overview of the composition and application of biomass ash. Part 1. Phase-mineral and chemical composition and classification. *Fuel* 2013;105:40–76. <https://doi.org/10.1016/j.fuel.2012.09.041>.
- [47] Vassilev SV, Baxter D, Vassileva CG. An overview of the behaviour of biomass during combustion: Part II. Ash fusion and ash formation mechanisms of biomass types. *Fuel* 2014;117:152–83. <https://doi.org/10.1016/j.fuel.2013.09.024>.
- [48] Daley PJ, Williams O, Heng Pang C, Wu T, Lester E. The impact of ash pellet characteristics and pellet processing parameters on ash fusion behaviour. *Fuel* 2019;251:779–88. <https://doi.org/10.1016/j.fuel.2019.03.142>.
- [49] Garcia E, Liu H. Ilmenite as alternative bed material for the combustion of coal and biomass blends in a fluidised bed combustor to improve combustion performance and reduce agglomeration tendency. *Energy* 2022;239:121913. <https://doi.org/10.1016/j.energy.2021.121913>.
- [50] Afilaka D. Avoiding the sintering of coal fired shallow fluidised beds, Doctor of Engineering Thesis. UK: University of Nottingham; 2015.
- [51] Wei Y, Chen M, Li Q, Niu S, Li Y. Isothermal combustion characteristics of anthracite and spent coffee grounds briquettes. *J Therm Anal Calorim* 2018; 3456789. <https://doi.org/10.1007/s10973-018-7790-x>.
- [52] Namkung H, Lee YJ, Park JH, Song GS, Choi JW, Choi YC, et al. Blending effect of sewage sludge and woody biomass into coal on combustion and ash agglomeration behavior. *Fuel* 2018;225:266–76. <https://doi.org/10.1016/j.fuel.2018.03.109>.
- [53] Teixeira P, Lopes H, Gulyurtlu I, Lapa N, Abelha P. Evaluation of slagging and fouling tendency during biomass co-firing with coal in a fluidized bed. *Biomass Bioenergy* 2012;39:192–203. <https://doi.org/10.1016/j.biombioe.2012.01.010>.
- [54] Wang L, Skreiberg Ø, Becidan M, Li H. Sintering of rye straw ash and effect of additives. *Energy Procedia* 2014;61:2008–11. <https://doi.org/10.1016/j.egypro.2014.12.063>.
- [55] Pintana P, Tippayawong N. Predicting ash deposit tendency in thermal utilization of biomass. *Eng J* 2016;20:15–24. <https://doi.org/10.4186/ej.2016.20.5.15>.
- [56] Niu Y, Tan H, Wang X, Liu Z, Liu H, Liu Y, et al. Study on fusion characteristics of biomass ash. *Bioresour Technol* 2010;101:9373–81. <https://doi.org/10.1016/j.biortech.2010.06.144>.
- [57] Liu B, He Q, Jiang Z, Xu R, Hu B. Relationship between coal ash composition and ash fusion temperatures. *Fuel* 2013;105:293–300. <https://doi.org/10.1016/j.fuel.2012.06.046>.
- [58] Zhu Y, Zhang H, Niu Y, Xu H, Zhang X, Hui S, et al. Experiment Study on Ash Fusion Characteristics of Cofiring Straw and Sawdust. *Energy Fuels* 2018;32: 525–31. <https://doi.org/10.1021/acs.energyfuels.7b03104>.

- [59] Li QH, Zhang YG, Meng AH, Li L, Li GX. Study on ash fusion temperature using original and simulated biomass ashes. *Fuel Process Technol* 2013;107:107–12. <https://doi.org/10.1016/j.fuproc.2012.08.012>.
- [60] Li F, Fang Y. Modification of ash fusion behavior of lignite by the addition of different biomasses. *Energy Fuels* 2015;29:2979–86. <https://doi.org/10.1021/acs.energyfuels.5b00054>.
- [61] Shen M, Qiu K, Zhang L, Huang Z, Wang Z, Liu J. Influence of coal blending on ash fusibility in reducing atmosphere. *Energies* 2015;8:4735–54. <https://doi.org/10.3390/en8064735>.
- [62] Song WJ, Tang LH, Zhu XD, Wu YQ, Zhu ZB, Koyama S. Effect of coal ash composition on ash fusion temperatures. *Energy Fuels* 2010;24:182–9. <https://doi.org/10.1021/ef900537m>.
- [63] Link S, Yrjas P, Hupa L. Ash melting behaviour of wheat straw blends with wood and reed. *Renew Energy* 2018;124:11–20. <https://doi.org/10.1016/j.renene.2017.09.050>.
- [64] Kuprianov VI, Kaewklum R, Chakritthakul S. Effects of operating conditions and fuel properties on emission performance and combustion efficiency of a swirling fluidized-bed combustor fired with a biomass fuel. *Energy* 2011;36:2038–48. <https://doi.org/10.1016/j.energy.2010.05.026>.
- [65] Hrdlička J, Skopec P, Dlouhý T, Hrdlička F. Emission factors of gaseous pollutants from small scale combustion of biofuels. *Fuel* 2016;165:68–74. <https://doi.org/10.1016/j.fuel.2015.09.087>.
- [66] Moradian F, Pettersson A, Svärd SH, Richards T. Co-Combustion of Animal Waste in a Commercial Waste-to-Energy BFB Boiler. *Energies* 2013;6:6170–87. <https://doi.org/10.3390/en6126170>.
- [67] Karampinis E, Grammelis P, Agraniotis M, Violidakis I, Kakaras E. Co-Firing of Biomass with Coal in Thermal Power Plants: Technology Schemes, Impacts, and Future Perspectives. *WIREs. Energy Environ* 2014;3:384–99. <https://doi.org/10.1002/wene.100>.
- [68] Houshfar E, Skreiberg Ø, Todorović D, Skreiberg A, Løvås T, Jovović A, et al. NO_x emission reduction by staged combustion in grate combustion of biomass fuels and fuel mixtures. *Fuel* 2012;98:29–40. <https://doi.org/10.1016/j.fuel.2012.03.044>.
- [69] Liu X, Luo Z, Yu C, Jin B, Tu H. Release Mechanism of Fuel-N into NO_x and N₂O Precursors during Pyrolysis of Rice Straw. *Energies* 2018;11:520. <https://doi.org/10.3390/en11030520>.
- [70] Guo F, Zhong Z. Co-combustion of anthracite coal and wood pellets: Thermodynamic analysis, combustion efficiency, pollutant emissions and ash slagging. *Environ Pollut* 2018;239:21–9. <https://doi.org/10.1016/j.envpol.2018.04.004>.
- [71] Dahlquist E. *Technologies for Converting Biomass to useful Energy*. CRC Press; 2013.
- [72] Allesina G, Pedrazzi S, Allegretti F, Tartarini P. Spent coffee grounds as heat source for coffee roasting plants: Experimental validation and case study. *Appl Therm Eng* 2017;126:730–6. <https://doi.org/10.1016/j.applthermaleng.2017.07.202>.
- [73] Chi H, Pans MA, Sun C, Liu H. An investigation of lime addition to fuel as a countermeasure to bed agglomeration for the combustion of non-woody biomass fuels in a 20kWth bubbling fluidised bed combustor. *Fuel* 2019;240:349–61. <https://doi.org/10.1016/j.fuel.2018.11.122>.